Effect of Si Content in Electrode and SiO_2 Additions to the Slag during Electroslag Remelting

Paul Jablonski, Martin Detrois*

National Energy Technology Laboratory, 1450 Queen Ave SW, Albany, OR 97321, USA

*E-mail: martin.detrois@netl.doe.gov

Abstract. Evolution of Si concentration in 316 stainless steel electrodes was observed during a melting campaign consisting of recycling electroslag remelted (ESR) ingots to make new electrodes using vacuum induction melting (VIM). This campaign consisted of iterations of VIM + ESR operations to optimize melting parameters. The effect of Si content on the melt parameters and ingot quality was further evaluated and additions of SiO_2 to the slag chemistry were studied using research-scale experiments, x-ray diffraction (XRF), combustion analysis, visual inspections, and computational tools. The Si concentration was found to decrease by approximately 600 ppm following ESR of 68 kg research-scale electrodes. Eventually, this led to failure of the slag skin and direct ingot/crucible contact. Additions of SiO_2 to the slag at levels matching the original calculated Si concentration in the electrode did not eliminate the slag skin failure and the current during steady state increased to maintain a constant melt rate. In this investigation, we propose a mechanism of slag skin failure consisting of local concentration of current density due to absence, or breakage, of the SiO_2 layer around the molten metal drop during ESR. This theory was reinforced by additional experiments in which Nb was added to the electrode to change the structure of the oxide layer around the drops.

1. Introduction

Advanced Ni and Fe based alloys are utilized in a variety of conditions such as aerospace, chemical processing, and power plants for electricity generation [1-4]. In these applications they need to overcome environmental attack, resist long term deformation (i.e., creep), and be able to survive cyclic conditions including temperature and stress cycles among other concerns. In order to ensure their lifetime performance, in some cases required for tens of years [4], a high degree of attention must be paid to their manufacture, which typically starts with melting. For aerospace applications, heats of metal are often melted several times using different techniques each aimed at addressing a certain aspect of the final alloy product quality [5]. For example, vacuum induction melting (VIM) is often used as a first operation to combine the complex assortment of alloy constituents and partially de-gas the alloy [5-7]. Electroslag remelting (ESR) is often used as a second operation to further refine the alloy and can be used to strip out unwanted contaminants such as S and P as well as remove oxide inclusions that can come from VIM operations [5, 8-9]. Vacuum arc remelting (VAR) is often used as a third operation to further strip out contained gasses such as oxygen, nitrogen, and hydrogen [5-6] as well as refine the microstructure in preparation for hot working.

During ESR, an electrode is heated past its melting point by a hot reactive slag (i.e., flux) typically consisting of CaF_2, CaO and Al_2O_3 with perhaps some additional minor oxide additions to control the final ingot chemistry or perhaps adjust the physical properties of the slag to better match the requirements of melting the particular alloy [8-11]. The slag is heated electrically as the AC current passes from the electrode through the slag and out the crucible [8-9]. Thus, during the melt this slag is situated between the forming ingot below and the melting electrode above. Typically, a "pre-fused" slag is used, i.e., one that has had the constituent oxides and fluorides melted together prior to use [8-9]. During melting, droplets of liquid metal travel from the electrode to the bottom of the crucible and form the ESR ingot. The droplets are superheated in the slag which favors reactions leading to refining of the alloy. The melt parameters are important in ensuring good melt control, steady state condition and efficiency of the process. Among those, the voltage, current and melt rate are of particular importance. In this investigation, a laboratory scale ESR furnace was used to study the remelting of 316 stainless steel that was repeatedly VIM then ESR melted in order to refine the startup and steady state operations of the ESR furnace. A decrease in the Si content was measured in the 316 stainless steel from the repeated iterations of VIM + ESR, as Si partially reported to the slag during ESR. In this investigation, the effect of the Si content in the electrode, and additions of SiO_2 to the slag, is discussed.

2. Experimental Procedure

Nominal 316 stainless steel chemistry bars (approximately 109 mm diameter) were utilized as electrodes and ESR melted into a 152 mm diameter crucible with a target melt rate of 1.5 kg/min (3.25 lb/min). The details of the furnace startup and operation can be found in Ref. [12]. The melts were made using 2.7 kg of pre-fused slag consisting primarily of CaF_2 – 30% CaO – 30% Al_2O_3. The complete slag chemistry is listed in Table 1. This provided a slag depth of approximately 50 mm between the electrode and the top of the forming ingot. Consarc 7th Generation furnace controls were utilized with melt voltage operated in voltage swing control and a target voltage swing setpoint of 0.8 V. Furnace operating conditions such as electrode weight, voltage and current were recorded every second. Melt rate was also recorded every second and was calculated by the vendor provided software over a 1 min time-period [13]. Total melt times were on the order of 60 min but varied depending on the electrode size, with steady state melting starting about 12 min after power on, utilizing a cold start [14]. Once melted, the ESR ingot was sectioned for chemistry analysis about 12 mm from the ingot top. Analysis consisted of X-ray fluorescence (XRF) on a Rigaku ZSX Primus II for major elements and combustion analysis on LECO systems for O, N, C, and S. Once sampled, the ingots and residual solid alloy pieces were combined with high quality melt stock by VIM melting and pouring to form a new electrode. The nominal target chemistry utilized was 17% Cr – 2.5% Mo – 11% Ni and < 0.06% C. Note that while 316 stainless steel typically contains Mn and Si, the specification is < 2.0% for each element and no minimum is specified thus no additions were made.

Table 1. Chemistry of the slag used for this investigation, provided by the vendor (wt.%).

CaF2	CaO	MgO	Al_2O_3	SiO_2	C	S	MnO_2	Fe	TiO_2	P	LOI
38.47	30.15	0.60	29.02	0.47	0.006	0.026	0.024	0.15	0.05	<0.01	0.015

Additions of SiO_2 to the slag were made in two ways. The first was to add SiO_2 to the top portion of the slag that was fed in during the cold start. The second way was to add the SiO_2 to the pre-fused slag in a resistance furnace heated to 1500°C for 1h thus making a new pre-fused slag composition.

3. Results and Discussion

The development of good melt control was ultimately successful as exhibited by the stable melt rate and swing and stable current and voltage typically observed (Figure 1). The composition of the electrode used to perform the ESR melt of Figure 1 is provided in Table 2. The silicon content in the electrode was measured to be 0.29%. A steady state condition of current at 2000 A and a voltage of about 33 V were typically observed. The 316 stainless steel ESR ingots were recycled into electrode stock by VIM with the addition of high quality remelt materials, as required to bring the melt back up to the target weight. It was observed that there were losses of Si as a result of the ESR process, typically on the order of 0.06%. With no Si additions made to the VIM melts, the Si in the 316 stainless steel eventually fell below the detection limit of the XRF (0.010%). Once the Si fell below the detection limit a more erratic current and voltage profile was always observed at some point during the melt which coincided with observed slag skin failure. For example, the recorded melt data for an electrode containing Si below the detection limit (Table 2) is provided in Figure 2a. The steady state current of low Si 316 stainless steel ESR melts would often approach or exceed 3000 A as the controller attempted to maintain the melt rate once slag skin failure occurred (Figure 2b). Since the slag skin failed locally, the most likely scenario was that the excess current went directly to the crucible at the site of slag skin failure. It has been proposed that Si (SiO_2) improves slag "lubricity" and thus lowers the tendency for slag skin failure [15]. Since some Si was reporting to the slag from the electrode it was conjectured that melts with low Si needed

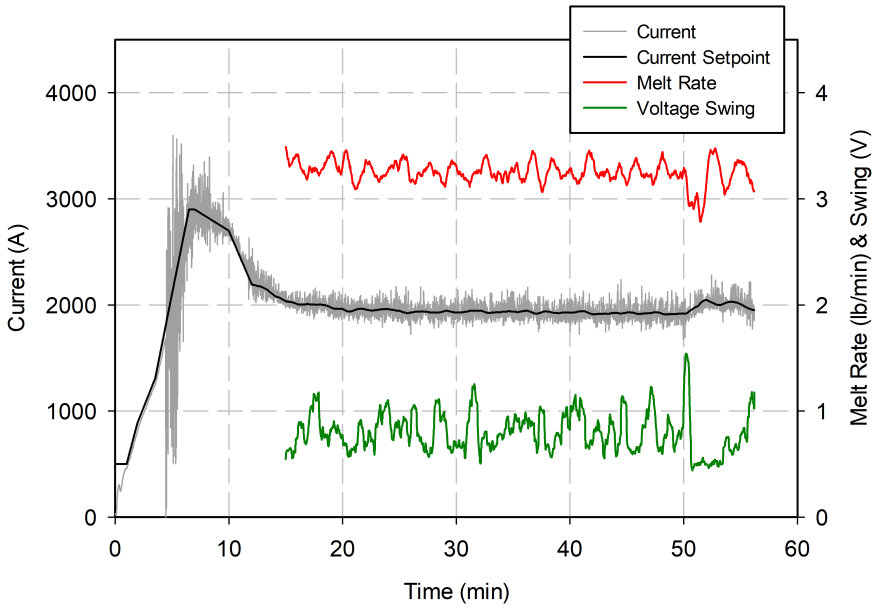

Figure 1. A typical melt with a nominal amount of Si in the alloy showing good melt control with stable melt rate and swing as well as stable current and voltage (not shown). (Melt rate and swing are only shown once steady state was reached.)

Table 2. Measured chemistry of the 316 electrodes after VIM (wt.%). Fe balanced.

Alloy (Fig. & ID)	Cr	Ni	Mo	Mn	Si	Cu	C	O	S
Fig. 1 (22-A35)	17.0	11.2	2.5	0.51	0.29	0.14	0.048	0.0016	0.0011
Fig. 2 (23-A63)	17.0	10.1	2.5	0.21	<0.010	0.07	0.036	0.0144	0.0007
Fig. 3 (22-A5)	17.0	11.5	2.6	0.28	0.06	0.09	0.052	0.0092	0.0028

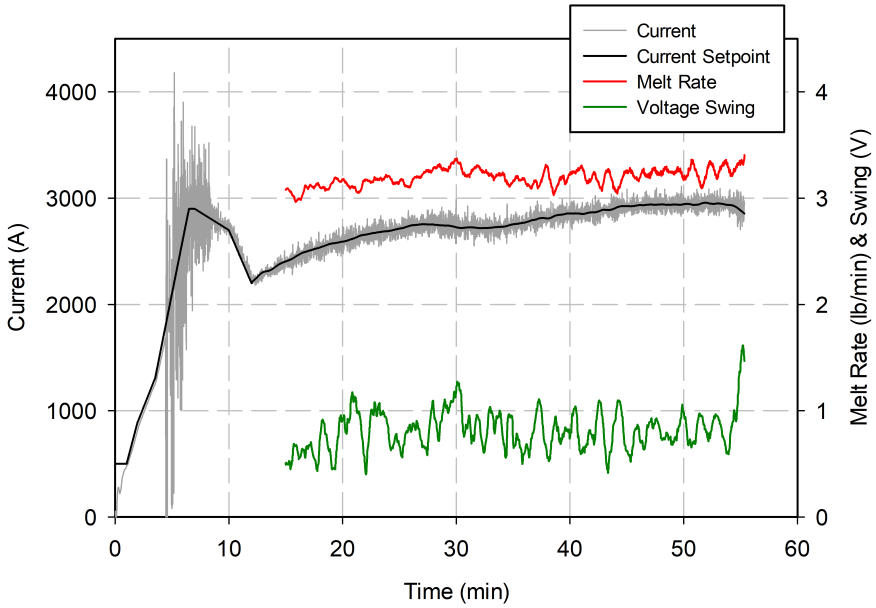

(a)

(b)

Figure 2. (a) A typical melt with low Si in the alloy showing reasonable melt control but the current never stabilizes and continues to rise to maintain the melt rate. (Melt rate and swing are only shown once "steady state" was reached.) (b) Slag skin failure was also typically observed.

an addition of SiO_2 to the slag. It was estimated that the transfer of Si from the electrode to the slag could result in substantial Si in the slag depending on the mass of electrode melted (on the order of ~2%). Thus, a series of experiments were run to add SiO_2 to the slag. The as-purchased pre-fused slag has a reported SiO_2 level of 0.47%. Experimentally, SiO_2 was added by two ways: adding SiO_2 to the last slag fed or by pre-fusing the flux with the addition of SiO_2. A total of 3 levels

of SiO_2 were added to the slag: 0.017, 0.17, and 1.6% which spanned about 3 orders of magnitude of SiO_2 for overall levels of 0.49, 0.64 and 2.1% SiO_2. For the pre-fused variant, 1.56% SiO_2 was added for an overall level of 2.02% SiO_2. In every melt with SiO_2 the slag skin failed, regardless of the level of SiO_2 added or the method of addition. In each case, the melt current was erratic leading us to conclude that the change in SiO_2 concentration in the slag (or lack of change) was not the source of the problem (Figure 3). However, a physical change in the slag was observed with all but the lowest additions of SiO_2 with the slag exhibiting a more friable nature. It should be noted that slag lubricity is more important in a moving collar type ESR mold rather than in our stationary crucible.

Since concluding that the slag chemistry was not the culprit for slag skin failure and excessive, erratic current observed, other considerations were made. During the ESR process, metal drips form, grow and are released from the electrode. The drips are pushed to the center of the electrode by the Lorentz force [16] effectively moving them away from the crucible sidewall. It is reasonable to expect that during melting, the drips form randomly on the surface of the electrode and that the metal surface would be oxidized to some extent. No attempt was made to capture and characterize a drip (it would be hard to freeze in the important in-situ structure) however it is

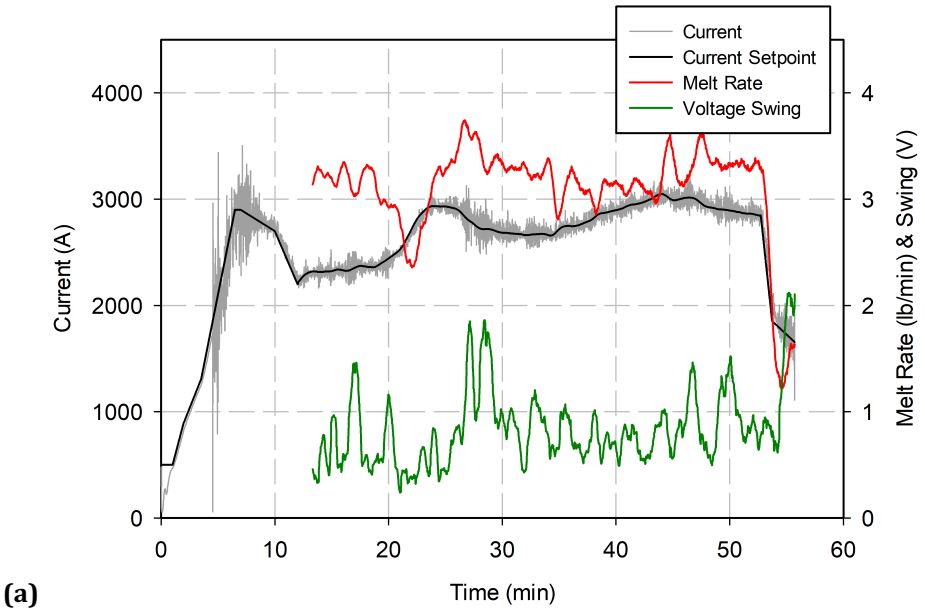

(a)

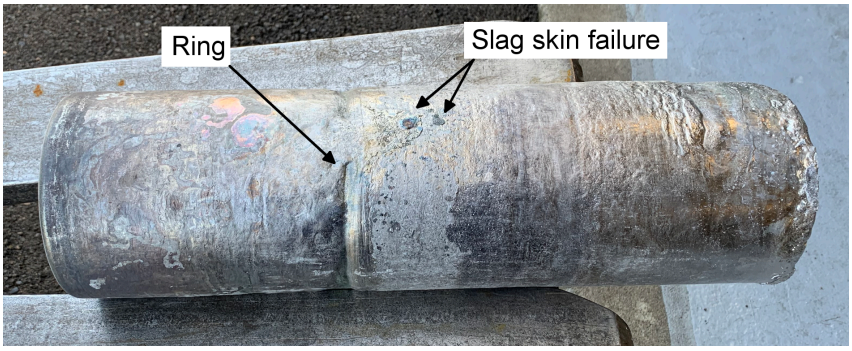

(b)

Figure 3. (a) A typical melt with low Si in the alloy with SiO_2 added to the slag showing a lack of melt and current control. Slag skin failure was also typically observed. (Melt rate and swing are only shown once "steady state" was reached.) (b) Resulting ESR ingot.

reasonable to expect that this structure will be similar to typical surface oxidation of stainless steel which consists of Cr/Mn spinel, then Cr oxide, then Si oxide traversing from the outer surface to the base metal (Figure 4). It is noteworthy that the Si oxide is known to be electrically resistive while the other two layers are conductive. Previous work, Ref. [17], has shown that a nearly continuous layer of SiO_2 forms at even very low levels of Si in the base metal.

It is theorized in this present work that, during ESR melting, a layer of SiO_2 will continue to form at the oxide/base metal interface even at very low levels of Si in the base metal (perhaps even those below the 0.010% detection limit). Furthermore, when a drip forms near the electrode edge, close to the sidewall, and grows sufficiently, it may "run out" of Si resulting in a locally high conducting drip segment (Figure 5) which could direct a substantial current to a small segment of the crucible resulting in the melting through the slag skin causing it to fail locally.

While Si typically forms a continuous oxide film at the oxide/base metal interface, the Nb containing alloy 441 stainless steel does not (even with ~0.3% Si, [18]). Instead, the Si and Nb are found dissolved into the Cr-rich oxide layer. Thus, it was further theorized that if SiO_2 forms a resistive layer on drips from the electrode and the Si occasionally "runs out" in low Si alloys, perhaps the problem can be alleviated by changing where the Si reports to in the oxide. The following experiment was conducted: Nb was added to 316 stainless steel during VIM at the level specified for 441 stainless steel (i.e., $\left(0.003 + 9 \times (\%C)\right)\%$ minimum, where $\%C$ is the concentration of C, to 0.9% maximum). The measured composition of the electrode is provided in Table 3. Both the Nb aim and measured amount in the VIM product were equal to 0.72%. A plot of the current, melt rate and swing for this ESR melt is shown in Figure 6. As can be seen in the

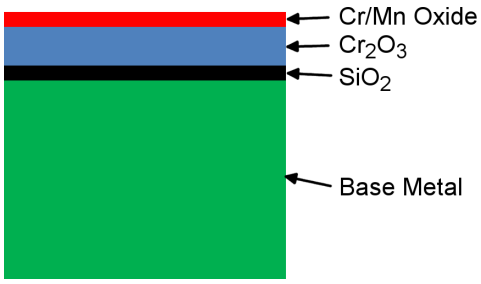

Figure 4. Schematic showing a cross section through typical surface oxidation of a stainless steel which consists of Cr/Mn spinel, then Cr oxide, then Si oxide traversing from the outer surface to the base.

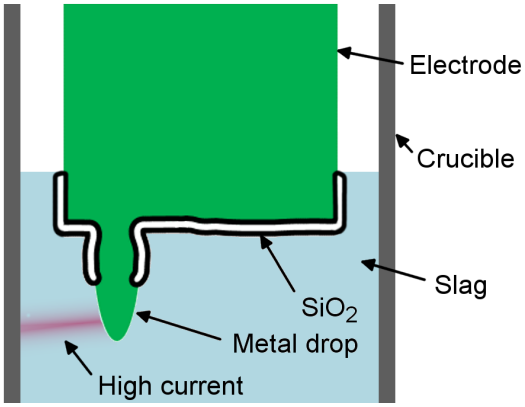

Figure 5. Schematic showing a cross section of an electrode with a growing metal drip. The Si oxide subscale that forms is shown in black. Note that it is proposed that the drip material "runs out" of Si and thus the Si oxide is absent from a portion of the drip. Other oxides are not show for simplicity.

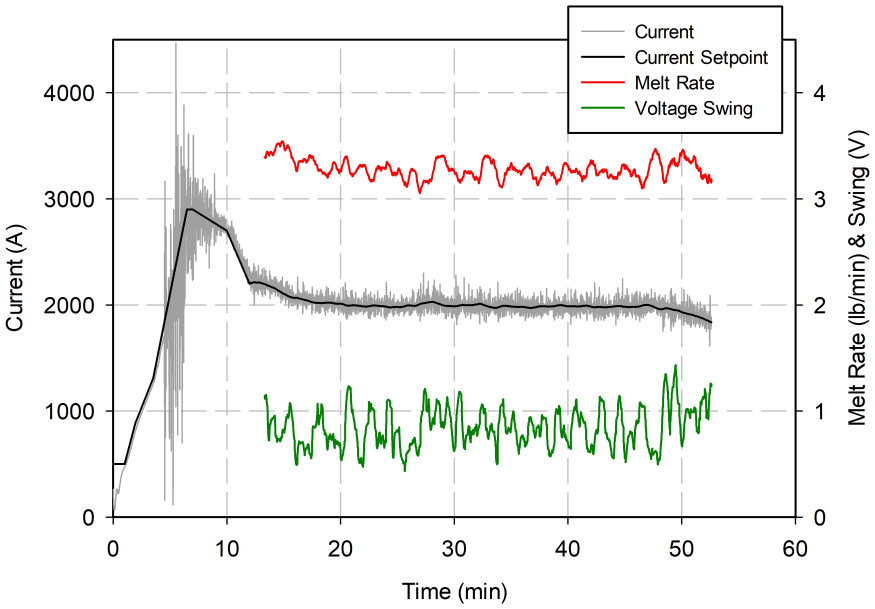

Figure 6. A plot of an ESR melt with Si <0.01% but Nb at 0.72%. Note that the melt exhibited good melt control with stable melt rate and swing as well as stable current and voltage (not shown). No slag skin breakthrough was observed. (Melt rate and swing are only shown once steady state was reached.)

Table 3. Measured chemistry of the 316 electrode/ingot after VIM/ESR (wt.%). Fe balanced.

Alloy (Fig. & ID)	Cr	Ni	Mo	Mn	Nb	Si	Cu	C	O
Fig. 6 (24-A5) VIM	17.1	9.9	2.5	0.16	0.72	<0.010	0.07	0.024	0.022
Fig. 6 (24-A6) ESR	17.2	9.9	2.5	0.16	0.53	<0.010	0.06	0.025	0.011

figure, there is good control of the melt rate and voltage swing. The current is also steady during the steady state portion of the melt at about 2000 A. These are all typical attributes of melts of 316 stainless steel when the alloy contains Si, however, this heat did not contain measurable Si but did contain 0.72% Nb. Thus, it seems that the Nb has modified where the Si oxide forms and no longer produces a resistive film that locally breaks down. It should be noted that a 26% decrease in the concentration of Nb was observed from the VIM electrode to the ESR ingot, as shown in Table 3. Such a drop in concentration has been observed in the past in the neighbor transition metal Ta in a ferritic/martensitic steel [19]. In this case, the loss of Ta was attributed to the formation of Ta-rich oxides during VIM that were subsequently removed during ESR, typically through absorption and dissolution in the slag [20]. If remelting campaigns are performed on the alloy of Figure 6/Table 3, it is expected that the Nb concentration will drop to levels sufficiently low to allow for the formation of a weak resistive film once again around the droplets during ESR.

Summary

In the work covered in this paper, it was observed that the level of Si in 316 stainless steel typically dropped by about 0.06 wt.% as a result of ESR melting. VIM consolidation melts were performed incorporating the ESR ingots with high quality remelt stock consisting of Fe, Ni, Cr and Mo, thus no additions of Si or Mn were made. As a result, the level of Si fell below the detection limit of 0.010 wt.%. When ESR melting these low Si heats of 316 stainless steel, slag skin failure and subsequent high current levels were observed during steady state. Modifying the slag chemistry with additions of SiO_2, either by pre-fusing the slag or by late additions of SiO_2 to the fed slag did not eliminate the slag skin failure. Previous work has shown that Si forms a continuous layer at the oxide/base metal interface. SiO_2 is an electrical insulator. In this work we propose a mechanism for slag skin failure in which metal drips form and run out of Si to form SiO_2 and thus concentrate the melt current locally in low Si melts of 316 stainless steel. If a drip is situated near the crucible wall, it is proposed that the concentrated current can sometimes cause the slag skin to remelt and thus cause the slag skin failure observed.

Previous research has shown that Nb can modify where Si is incorporated in the oxide and can eliminate the continuous layer of SiO_2. As part of this work, we added Nb to a VIM melt of 316 stainless steel. The ESR of this material showed good control of the current, melt rate and voltage swing and a lack of slag skin failure. Thus, it is proposed that the source of slag skin failure experienced on these small ESR heats was directly related to the concentration of current locally as a result of the low Si content.

Acknowledgments

This work was performed in support of the US Department of Energy's Fossil Energy and Carbon Management Office's Advanced Energy Materials Research Program and executed through the National Energy Technology Laboratory Research & Innovation Center (Advanced Energy Materials MYRP-1025034). The authors would like to thank Mr. Edward Argetsinger, Mr. Joseph Mendenhall, Mr. Christopher McKaig, and Mr. James Willis for assistance in melting.

References

[1] Viswanathan R *et al* 2005 *J Mater Eng Perf* **14** (3) 281
[2] Viswanathan R 2004 *Adv Mater Processes* **162** (8) 73
[3] Viswanathan R, Armor A F and Booras G 2004 *Power* **4** 42
[4] Hardy M C, Detrois M, McDevitt E T, Argyrakis C, Saraf V, Jablonski P D, Hawk J A, Buckingham R C, Kitaguchi H S and Tin S 2020 *Metall Mater Trans A* **51** (6) 2626
[5] Sims C T, Stoloff N S and Hagel W C 1987 *Superalloys II* (New York, NY: John Wiley & Sons)
[6] Choudhury A 1992 *ISIJ Int* **32** 563
[7] Simkovich A 1966 *J Met* **4** 504
[8] Duckworth W E and Hoyle G 1969 *Electroslag Refining* (New York, NY: Chapman and Hall)
[9] Hoyle G 1983 *Electroslag Processes, Principles and Practice* (London, UK: Applied Science Publishers)
[10] Mitchell A 1981 *Can Metall Q* **20** 101
[11] Detrois M and Jablonski P D 2017 *Proc Int Symp on Liquid Metal Processing & Casting (LMPC 2017)* p 75
[12] Jablonski P D, Cretu M and Nauman J 2017 *Proc Int Symp on Liquid Metal Processing & Casting (LMPC 2017)* p 157
[13] Private communication with Miller C April 7th, 2022
[14] Detrois M and Jablonski P D 2022 *Proc Int Symp on Liquid Metal Processing & Casting (LMPC 2022)* p 309
[15] Shi C, Li J, Cho J, Jiang F and Jung I 2015 *Metall Mater Trans B* **46** 2110
[16] Shi H, Tu M, Chen Q and Shen H 2020 *Int J Heat Mass Transfer* **158** 119713
[17] Jablonski P D and Sears J 2013 *J Power Sources* **228** 141
[18] Jablonski P D, Cowen C J and Sears J 2010 *J Power Sources* **195** 813
[19] Detrois M, Jablonski P D and Hawk J A 2019 *Metall Mater Trans B* **50** (4) 1686
[20] Dong Y, Jiang Z, Cao Y, Yu A and Hou D 2014 *Metall Mater Trans B* **45** 1315